Distribution of AoI in EH-powered Multi-source Systems under Non-preemptive and Preemptive Policies

Mohamed A. Abd-Elmagid and Harpreet S. Dhillon

***Abstract*—In this paper, we study a *multi-source* updating system in which a transmitter powered by energy harvesting (EH) has multiple sources generating status updates about several physical processes. The status updates are then sent to a destination node where the freshness of each status update is measured in terms of *Age of Information (AoI)*. The harvested energy packets and the status updates of each source are assumed to arrive at the transmitter according to independent Poisson processes, and the service time of each status update is assumed to be exponentially distributed. We focus on understanding the *distributional properties* of AoI under *both non-preemptive and preemptive in service queueing disciplines* at the transmitter. In particular, we use the stochastic hybrid systems (SHS) framework to derive closed-form expressions of the moment generating function (MGF) and average AoI under each queueing discipline. To the best of our knowledge, this paper is the first to characterize the AoI performance in EH-powered multi-source updating systems under both non-preemptive and preemptive queueing models. The generality of our results is demonstrated by recovering several existing results as special cases. Our results reveal a fundamental trade-off between obtaining a minimum sum of average AoI values associated with different sources (average sum-AoI) and achieving fairness among the average AoI values of different sources. They also reveal the impact of system design parameters on the achievable AoI performance.**

***Index Terms*—Age of information, energy harvesting, queueing systems, communication networks, stochastic hybrid systems.**

I. Introduction

Timely delivery of real-time status updates is crucial in numerous Internet of Things (IoT)-enabled updating systems, where a *transmitter node* aims to maintain the freshness of information at a *destination node* about some physical process(es) of interest [1]. This has motivated the study of AoI as a performance metric quantifying the freshness of information at the destination [2]. The authors of [2] derived the average AoI for single-source systems in which *a non-EH transmitter* (i.e., it is powered by a reliable energy source) has a single source of information. This inspired significant follow-up work on the analysis of AoI in single-source systems. However, the analysis of AoI in multi-source systems is quite challenging because of which the prior work in this direction is relatively sparse [3]–[7]. For multi-source systems, the average AoI was characterized under non-preemptive and preemptive in service/waiting queueing disciplines in [3]–[6], whereas the distribution of AoI was numerically characterized for various discrete time queues in [7]. Different from [2]–[7] that considered a non-EH transmitter, our focus in this paper is on the analytical characterization of the distributional properties of AoI in EH-powered multi-source systems.

A salient feature of the analyses in the above works was their reliance on identifying the properties of the AoI sample functions and applying geometric arguments. Since these approaches often involve tedious calculations of joint moments, the authors of [8] and [9] aimed at developing an alternative approach for the queueing-theoretic analyses of AoI by building on the SHS framework of [10]. Following [8], [9], the SHS approach was then used to evaluate the average AoI for a variety of queueing disciplines in [11]–[13], and the MGF of AoI for a two-source system with status update management in [14]. Compared to the analyses of [11]–[14] that considered a non-EH transmitter, the analysis of AoI using the SHS approach becomes much more challenging when we consider an EH-powered transmitter. This is because the process of decision-making (i.e., the decisions of discarding or serving new arriving status updates at the transmitter) is dependent on the joint evolution of the battery state and the system occupancy with respect to the status updates.

For the case where the transmitter is powered by EH, there are a handful of prior works [15]–[20] analyzing AoI by applying geometric arguments [15], [16], and by using the SHS approach [17]–[20]. However, the analyses of [15]–[19] have been limited to the evaluation of the average AoI in single-source systems, and the analysis of [20] was focused on the characterization of the distributional properties of AoI in single-source systems. Different from these, this paper makes the first attempt at deriving the MGF/average of AoI in multi-source updating systems powered by EH. Before going into more details about our contributions, it is instructive to note that besides the above queueing theory-based analyses of AoI, there have also been efforts to optimize AoI or some other AoI-related metrics in different EH-powered communication systems that deal with time-sensitive information [21]–[25].

Contributions. This paper presents a novel queueing-theoretic analysis to derive closed-form expressions for the MGF/average of AoI in EH-powered multi-source systems under both non-preemptive and preemptive in service queueing disciplines. In our analysis, we use the SHS framework where the system discrete state is modeled as a two-dimensional continuous-time Markov chain (CTMC) to track both the numbers of update and harvested energy packets in the system. Our asymptotic results demonstrate the generality of the expressions derived in this paper by recovering several existing results for single source-systems with an EH-powered transmitter [20], and for multi-source systems with a non-EH transmitter [8]. Our numerical results demonstrate the importance of incorporating the higher moments of AoI in the implementation/optimization of multi-source updating systems rather than just relying on its average.

II. System Model

A. Network Model

We consider a real-time updating system in which an EH-powered transmitter observes N physical processes, and sends

The authors are with Wireless@VT, Department of ECE, Virginia Tech, Blacksburg, VA. Email: {maelaziz, hdhillon}@vt.edu. The support of the U.S. NSF (Grants CPS-1739642 and CNS-1814477) is gratefully acknowledged.

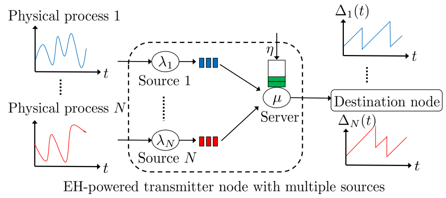

Fig. 1. An illustration of the system setup.

its measurements to a destination in the form of status update packets. As shown in Fig. 1, the transmitter consists of N sources and a single server; each source generates status updates about one physical process, and the server delivers the status updates generated from all the sources to the destination. In particular, each status update packet generated by source i carries some information about the value of the i-th physical process and a time stamp indicating the time at which that process was sampled. This system setup can be mapped to many scenarios of practical interest, such as an IoT network in which an aggregator (represents the transmitter in our model) delivers measurements sensed/generated by the N IoT devices (represent the sources) in its vicinity to a destination.

Status update packets generated by the i-th source are assumed to follow a Poisson process with rate λ_i. Further, the energy packets are assumed to arrive at the transmitter according to a Poisson process with rate η, and are stored in a battery queue of length B packets at the server (for serving the update packets generated by the different sources). We consider that each energy packet contains the energy required for sending one status update from any of the sources [15]–[19], and hence the length of the energy battery queue reduces by one whenever a status update is successfully received at the destination. Given that the transmitter node has at least one energy packet in its battery queue, the time needed by its server to send a status update packet is assumed to be a rate μ exponential random variable [2]–[4]. Let $\rho = \frac{\lambda}{\mu}$ and $\beta = \frac{\eta}{\mu}$ respectively denote the server utilization and energy utilization factors, where $\lambda = \sum_{i=1}^{N} \lambda_i$. Further, we have $\rho_i = \frac{\lambda_i}{\mu}$, $\lambda_{-i} = \sum_{j=1,\, j\neq i}^{N} \lambda_j$, and $\rho_{-i} = \frac{\lambda_{-i}}{\mu}$.

We quantify the freshness of information about each physical process at the destination (as a consequence of receiving status update packets from the transmitter) using the concept of AoI. Formally, AoI is defined as follows [2].

Definition 1. *Let $t_{i,k}$ denote the arrival time instant of the k-th update of source i at the transmitter. Further, define $L_i(t)$ to be the index of the source i's latest update received at the destination by time t. Then, the AoI associated with the physical process observed by source i at the destination (referred henceforth as the AoI of source i) is defined as the following random process: $\Delta_i(t) = t - t_{i,L_i(t)}$.*

B. Queueing Disciplines Considered in This Paper

For the above system setup, we analyze the AoI performance at the destination under two different queueing disciplines for managing update packet arrivals at the transmitter node. These queueing disciplines are described next.

Last-come-first-served without preemption (LCFS-WP). Under this queueing discipline, a new arriving update packet at the transmitter (from any of the sources) enters service upon its arrival if the server is idle (i.e., there is no update packet in service) and the battery contains at least one energy packet; otherwise, the new arriving update packet is discarded.

Last-come-first-served with preemption in service (LCFS-PS). When the server is idle, the management of a new arriving update packet under this queueing discipline is similar to the LCFS-WP one. However, when the server is busy, a new arriving update packet replaces[1] the current packet being served and the old packet in service is discarded.

With regards to the EH process, we consider that the transmitter can harvest energy only if its server is idle. This case corresponds to the scenario where the transmitter is equipped with a single radio frequency chain, and thus can either transmit a status update or harvest energy at a certain time instant. The case where the transmitter can harvest energy anytime (i.e., even when its server is busy) is left as a promising direction of future work.

III. Problem Statement and Solution Approach

Our goal is to analytically characterize the AoI performance of each source at the destination node as a function of: i) the rates of generating status update packets by the N sources $\{\lambda_i\}$, ii) the rate of harvesting energy packets η, iii) the rate of serving status update packets μ, and iv) the finite capacity of the energy battery queue B, at the transmitter node. Unlike most of the analyses of AoI in the existing literature which were focused on deriving its average, our analysis is focused on deriving distributional properties of AoI through the characterization of its MGF. To derive the MGF of AoI for the considered queueing disciplines at the transmitter node (presented in Subsection II-B), we resort to the SHS framework in [10], which was first tailored for the analysis of AoI in [8] and [9]. In the following, we provide a very brief[2] introduction of the SHS framework, which will be useful in understanding our AoI MGF analysis in the next section.

The SHS is represented by a hybrid state $(q(t), \mathbf{x}(t))$, where $q(t) \in \mathcal{Q} = \{1, \cdots, m\}$ is a finite-state CTMC modeling the system discrete state and $\mathbf{x}(t) = [x_0(t), \cdots, x_n(t)] \in \mathbb{R}^{1\times(n+1)}$ describes the evolution of the system continuous state over time. In the CTMC $q(t)$, a transition $l \in \mathcal{L}$ from state q_l to state q_l' occurs with a rate $\lambda^{(l)}\delta_{q_l,q(t)}$ and causes $\mathbf{x}$ to reset to $\mathbf{x}' = \mathbf{x}\mathbf{A}_l$, where $\mathbf{A}_l \in \mathbb{B}^{(n+1)\times(n+1)}$ is a binary reset map matrix and the Kronecker delta function $\delta_{q_l,q(t)}$ ensures that l occurs only when $q(t) = q_l$. Further, $\dot{\mathbf{x}}(t) \triangleq \dfrac{\partial \mathbf{x}(t)}{\partial t} = \mathbf{1}$ holds as long as the state $q(t)$ is unchanged, where $\mathbf{1}$ is the row vector $[1, \cdots, 1] \in \mathbb{R}^{1\times(n+1)}$. Denote by $\mathcal{L}_q' = \{l \in \mathcal{L} : q_l' = q\}$ and $\mathcal{L}_q = \{l \in \mathcal{L} : q_l = q\}$ the sets of incoming and outgoing transitions for state q. Further, let $\mathbf{v}_q(t) = [v_{q0}(t), \cdots, v_{qn}(t)] \in \mathbb{R}^{1\times(n+1)}$ denote the correlation vector between $q(t)$ and $x(t)$, and $\mathbf{v}_q^s(t) = [v_{q0}^s(t), \cdots, v_{qn}^s(t)] \in \mathbb{R}^{1\times(n+1)}$ denote the correlation vector

[1] Our analysis is extended in the journal expansion of this paper [26] to the source-aware preemption in service queueing discipline, which only allows preemption between the status updates generated by the same source to enhance fairness.

[2] Interested readers are advised to refer to [8] and [9] for a detailed discussion about the use of the SHS approach in the analysis of AoI.

between $q(t)$ and the exponential function $e^{s\mathbf{x}(t)}$, where $s \in \mathbb{R}$. Thus, we have

$$\mathbf{v}_q(t) = [v_{q0}(t), \cdots, v_{qn}(t)] = \mathbb{E}[\mathbf{x}(t)\delta_{q,q(t)}],\ \forall q \in \mathcal{Q}, \quad (1)$$

$$\mathbf{v}_q^s(t) = [v_{q0}^s(t), \cdots, v_{qn}^s(t)] = \mathbb{E}[e^{s\mathbf{x}(t)}\delta_{q,q(t)}],\ \forall q \in \mathcal{Q}. \quad (2)$$

Using the above notations, it has been shown in [9, Theorem 1] that under the ergodicity assumption of the CTMC $q(t)$, if we can find a non-negative limit $\bar{\mathbf{v}}_q = [\bar{v}_{q0}, \cdots, \bar{v}_{qn}]$, $\forall q \in \mathcal{Q}$, for the correlation vector $\mathbf{v}_q(t)$ satisfying

$$\bar{\mathbf{v}}_q \sum_{l \in \mathcal{L}_q} \lambda^{(l)} = \bar{\pi}_q \mathbf{1} + \sum_{l \in \mathcal{L}'_q} \lambda^{(l)} \bar{\mathbf{v}}_{q_l} \mathbf{A}_l,\ q \in \mathcal{Q}, \quad (3)$$

where $\bar{\pi} = [\bar{\pi}_0, \cdots, \bar{\pi}_m]$ is the unique state stationary vector satisfying

$$\bar{\pi}_q \sum_{l \in \mathcal{L}_q} \lambda^{(l)} = \sum_{l \in \mathcal{L}'_q} \lambda^{(l)} \bar{\pi}_{q_l},\ q \in \mathcal{Q},\ \sum_{q \in \mathcal{Q}} \bar{\pi}_q = 1, \quad (4)$$

then:

- The expectation of $x(t)$, $\mathbb{E}[x(t)]$, converges to the following stationary vector:
$$\mathbb{E}[x] = \sum_{q \in \mathcal{Q}} \bar{\mathbf{v}}_q. \quad (5)$$
- There exists $s_0 > 0$ such that for all $s < s_0$, $\mathbf{v}_q^s(t)$ converges to $\bar{\mathbf{v}}_q^s$ that satisfies
$$\bar{\mathbf{v}}_q^s \sum_{l \in \mathcal{L}_q} \lambda^{(l)} = s\bar{\mathbf{v}}_q^s + \sum_{l \in \mathcal{L}'_q} \lambda^{(l)} [\bar{\mathbf{v}}_{q_l}^s \mathbf{A}_l + \bar{\pi}_{q_l} \mathbf{1} \hat{\mathbf{A}}_l],\ q \in \mathcal{Q}, \quad (6)$$

where $\hat{\mathbf{A}}_l \in \mathbb{B}^{(n+1)\times(n+1)}$ is a binary matrix whose elements are constructed as: $\hat{\mathbf{A}}_l(k,j) = 1$ if $k = j$ and the j-th column of $\mathbf{A}_l$ is a zero vector; otherwise, $\hat{\mathbf{A}}_l(k,j) = 0$. Further, the MGF of the state $\mathbf{x}(t)$, which can be obtained as $\mathbb{E}[e^{s\mathbf{x}(t)}]$, converges to the following stationary vector:

$$\mathbb{E}[e^{s\mathbf{x}}] = \sum_{q \in \mathcal{Q}} \bar{\mathbf{v}}_q^s. \quad (7)$$

From (5) and (7), when the first element of the continuous state $\mathbf{x}(t)$ represents the AoI at the destination node, the expectation and the MGF of AoI at the destination node respectively converge to:

$$\Delta_1 = \sum_{q \in \mathcal{Q}} \bar{v}_{q0}, \quad (8)$$

$$M(s) = \sum_{q \in \mathcal{Q}} \bar{v}_{q0}^s. \quad (9)$$

IV. Analysis of the MGF of AoI

From [9, Theorem 1] (stated in Section III), we note that the use of (6) to derive the MGF of AoI requires finding a non-negative limit $\bar{\mathbf{v}}_q$ ($\forall q \in \mathcal{Q}$) satisfying (3). In the expanded journal version of this paper [26] (Theorems 1 and 2), we have rigorously shown the existence of a non-negative $\bar{\mathbf{v}}_q$ satisfying (3) under each queueing discipline. Note that the solution of the equations in (3) can be obtained along the same lines of the analysis presented in this paper for solving the equations in (6). Thus, for the sake of brevity, we next focus on evaluating $\bar{v}_{q0}^s, \forall q \in \mathcal{Q}$, satisfying (6), using which the MGF of AoI under each queueing discipline is obtained as in (9).

Without loss of generality, we consider that source 1 is the source of interest in the AoI analysis in the sequel. As will be

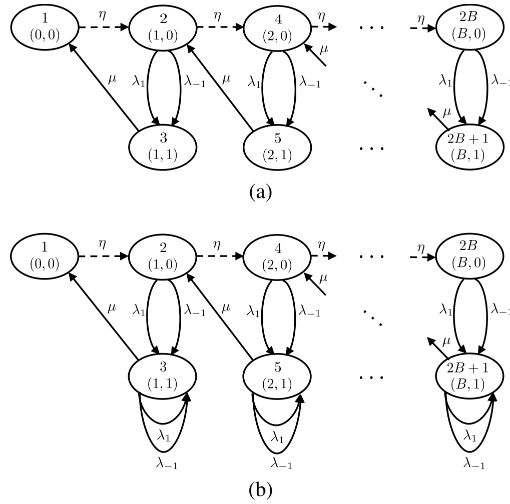

Fig. 2. Markov chains modeling the discrete state of the system: (a) LCFS-WP queueing discipline, and (b) LCFS-PS queueing discipline.

evident shortly, one can then use the same expressions derived for source 1 to characterize the AoI performance of the other sources. While analyzing the AoI performance of source 1, the status update packets generated by the other sources follow a Poisson process with rate $\lambda_{-1} = \sum_{j=2}^{N} \lambda_j$. Further, the continuous process $\mathbf{x}(t)$ is expressed as $\mathbf{x}(t) = [x_0(t), x_1(t)]$, where $x_0(t)$ represents the source 1's AoI at the destination (i.e., $\Delta_1(t)$), and $x_1(t)$ tracks the value that will be assigned to the source 1's AoI when the current packet in service is received at the destination. Recall from Section III that the elements of $\mathbf{x}(t)$ increase linearly with time as long as there is no change in $q(t)$.

A. LCFS-WP Queueing Discipline

The CTMC modeling the discrete state of the system $q(t) \in \mathcal{Q}$ under the LCFS-WP queueing discipline is depicted in Fig. 2a. Each state in $\mathcal{Q}$ represents a potential combination of the number of update packets in the system and the number of energy packets in the battery queue at the server. For instance, a state $q = (e_q, u_q)$ indicates that the system has u_q status update packets and the energy battery queue at the server contains e_q energy packets. Note that since the system can have at most one status update packet at any time instant in the LCFS-WP queueing discipline and there is no need to track the source index from which the update packet in service was generated, we have $u_q \in \{0, 1\}$. In particular, $u_q = 0$ indicates that the system is empty and hence the server is idle, and $u_q = 1$ indicates that the server is serving the existing update packet in the system. Since the battery queue at the server has a capacity of B packets, we have $e_q \in \{0, 1, \cdots, B\}$. We denote the set of states in the $i-$th row of the Markov chain by r_i. Further, Table I presents the set of different transitions $\mathcal{L}$ and their impact on the values of both $q(t)$ and $\mathbf{x}(t)$. Before proceeding into evaluating $\bar{\mathbf{v}}_q^s$, $\forall q \in \mathcal{Q}$, satisfying (6), we first describe the set of transitions as follows.

$l = 4k - 3$: This subset of transitions takes place between the states of the Markov chain in r_1, corresponding to the time when the system is empty. In particular, a transition from this set of transitions occurs when a new energy packet is harvested by the transmitter. Clearly, since harvesting a

TABLE I
TRANSITIONS OF THE LCFS-WP QUEUEING DISCIPLINE IN FIG. 2A ($2 \leq k \leq B$).

l	$q_l \to q_l'$	$\lambda^{(l)}$	$\mathbf{x}\mathbf{A}_l$	$\mathbf{A}_l$	$\hat{\mathbf{A}}_l$	$\bar{\mathbf{v}}_{q_l}\mathbf{A}_l$	$\bar{\pi}_{q_l}\mathbf{1}\hat{\mathbf{A}}_l$
1	$1 \to 2$	η	$[x_0, 0]$	$\begin{bmatrix}1 & 0\\0 & 0\end{bmatrix}$	$\begin{bmatrix}0 & 0\\0 & 1\end{bmatrix}$	$[\bar{v}_{10}, 0]$	$[0, \bar{\pi}_1]$
2	$2 \to 3$	λ_1	$[x_0, 0]$	$\begin{bmatrix}1 & 0\\0 & 0\end{bmatrix}$	$\begin{bmatrix}0 & 0\\0 & 1\end{bmatrix}$	$[\bar{v}_{20}, 0]$	$[0, \bar{\pi}_2]$
3	$2 \to 3$	λ_{-1}	$[x_0, x_0]$	$\begin{bmatrix}1 & 1\\0 & 0\end{bmatrix}$	$\begin{bmatrix}0 & 0\\0 & 0\end{bmatrix}$	$[\bar{v}_{20}, \bar{v}_{20}]$	$[0, 0]$
4	$3 \to 1$	μ	$[x_1, 0]$	$\begin{bmatrix}0 & 0\\1 & 0\end{bmatrix}$	$\begin{bmatrix}0 & 0\\0 & 1\end{bmatrix}$	$[\bar{v}_{31}, 0]$	$[0, \bar{\pi}_3]$
$4k-3$	$2k-2 \to 2k$	η	$[x_0, 0]$	$\begin{bmatrix}1 & 0\\0 & 0\end{bmatrix}$	$\begin{bmatrix}0 & 0\\0 & 1\end{bmatrix}$	$[\bar{v}_{2k-2,0}, 0]$	$[0, \bar{\pi}_{2k-2}]$
$4k-2$	$2k \to 2k+1$	λ_1	$[x_0, 0]$	$\begin{bmatrix}1 & 0\\0 & 0\end{bmatrix}$	$\begin{bmatrix}0 & 0\\0 & 1\end{bmatrix}$	$[\bar{v}_{2k,0}, 0]$	$[0, \bar{\pi}_{2k}]$
$4k-1$	$2k \to 2k+1$	λ_{-1}	$[x_0, x_0]$	$\begin{bmatrix}1 & 1\\0 & 0\end{bmatrix}$	$\begin{bmatrix}0 & 0\\0 & 0\end{bmatrix}$	$[\bar{v}_{2k,0}, \bar{v}_{2k,0}]$	$[0, 0]$
$4k$	$2k+1 \to 2k-2$	μ	$[x_1, 0]$	$\begin{bmatrix}0 & 0\\1 & 0\end{bmatrix}$	$\begin{bmatrix}0 & 0\\0 & 1\end{bmatrix}$	$[\bar{v}_{2k+1,1}, 0]$	$[0, \bar{\pi}_{2k+1}]$

TABLE II
TRANSITIONS OF THE LCFS-PS QUEUEING DISCIPLINE IN FIG. 2B ($2 \leq k \leq B$).

l	$q_l \to q_l'$	$\lambda^{(l)}$	$\mathbf{x}\mathbf{A}_l$	$\mathbf{A}_l$	$\hat{\mathbf{A}}_l$	$\bar{\mathbf{v}}_{q_l}\mathbf{A}_l$	$\bar{\pi}_{q_l}\mathbf{1}\hat{\mathbf{A}}_l$
$4B+2k-3$	$2k-1 \to 2k-1$	λ_1	$[x_0, 0]$	$\begin{bmatrix}1 & 0\\0 & 0\end{bmatrix}$	$\begin{bmatrix}0 & 0\\0 & 1\end{bmatrix}$	$[\bar{v}_{2k-1,0}, 0]$	$[0, \bar{\pi}_{2k-1}]$
$4B+2k-2$	$2k-1 \to 2k-1$	λ_{-1}	$[x_0, x_0]$	$\begin{bmatrix}1 & 1\\0 & 0\end{bmatrix}$	$\begin{bmatrix}0 & 0\\0 & 0\end{bmatrix}$	$[\bar{v}_{2k-1,0}, \bar{v}_{2k-1,0}]$	$[0, 0]$

new energy packet does not impact the value of $\Delta_1(t)$, we observe that the first element in the updated value of the age vector $\mathbf{x}\mathbf{A}_l$ (as a consequence of this transition) is x_0, i.e., this transition does not induce any change in the source 1's AoI at the destination. Further, since the server is idle in the states of r_1, the second component of $\mathbf{x}(t)$ (quantifying the age of the source 1's packet in service, if any) becomes irrelevant for such set of states. Note that whenever a component of $\mathbf{x}(t)$ is/becomes irrelevant after the occurrence of some transition l, its value in the updated age vector $\mathbf{x}\mathbf{A}_l$ can be set arbitrarily (except for $l = 4k-1$, as will be clear shortly). Following the convention [8], we set the value corresponding to such irrelevant components in the updated age value to 0, and thus we observe that the second component of $\mathbf{x}\mathbf{A}_{4k-3}$ is 0.

$l = 4k-2$: A transition from this subset of transitions occurs when there is a new arriving update packet of source 1 at the transmitter node. Since the age of this new arriving update packet at the transmitter is 0 and it does not have any impact on $\Delta_1(t)$, we note that the updated age vector $\mathbf{x}\mathbf{A}_{4k-2}$ is set to be $[x_0, 0]$.

$l = 4k-1$: A transition from this subset of transitions occurs when any of the sources other than source 1 generates a new update packet at the transmitter node. We note that the first component of $\mathbf{x}\mathbf{A}_{4k-1}$ is x_0 since this transition does not have any impact on $\Delta_1(t)$. Further, to ensure that the value of $\Delta_1(t)$ does not change when this new arriving update packet is received by the destination, we set the second component of $\mathbf{x}\mathbf{A}_{4k-1}$ to x_0, i.e., the value of the source 1's AoI at the arrival instant of this new update packet.

$l = 4k$: This subset of transitions occurs when the update packet in service is delivered to the destination. When the update packet received at the destination belongs to source 1, the AoI of source 1 is reset to its age; otherwise, the AoI of source 1 does not change. Note that the latter case is achieved by setting the second component of $\mathbf{x}\mathbf{A}_{4k-1}$ to x_0. In addition, since the system becomes empty after the occurrence of this transition, the second component of the age vector $\mathbf{x}(t)$ becomes irrelevant, and thus its corresponding value in the updated age vector $\mathbf{x}\mathbf{A}_{4k}$ is 0.

To obtain $\bar{\mathbf{v}}_q^s$ satisfying (6), we need to compute the state probabilities $\{\bar{\pi}_q\}$, and the vectors $\bar{\mathbf{v}}_{q_l}^s\mathbf{A}_l$ and $\bar{\pi}_{q_l}\mathbf{1}\hat{\mathbf{A}}_l$. The calculations of $\bar{\mathbf{v}}_{q_l}^s\mathbf{A}_l$ and $\bar{\pi}_{q_l}\mathbf{1}\hat{\mathbf{A}}_l$ are listed in Table I, and $\{\bar{\pi}_q\}$ are given by the following proposition.

Proposition 1. *The steady state probabilities $\{\bar{\pi}_q\}$ can be expressed as*

$$\bar{\pi}_{2k} = \left(\frac{\beta}{\rho}\right)^k \bar{\pi}_1, \tag{10}$$

$$\bar{\pi}_{2k+1} = \rho\left(\frac{\beta}{\rho}\right)^k \bar{\pi}_1, \tag{11}$$

where $1 \leq k \leq B$ and $\bar{\pi}_1$ is given by

$$\bar{\pi}_1 = \begin{cases} \dfrac{1}{1 + B(1+\rho)}, & \text{if } \rho = \beta, \\ \dfrac{\rho^B(\beta - \rho)}{\rho^B(\beta-\rho) + \beta(1+\rho)(\beta^B - \rho^B)}, & \text{otherwise.} \end{cases} \tag{12}$$

Proof: The expressions in (10)-(12) follow from solving the set of equations in (4). A detailed proof can be found in Appendix A of [20]. ∎

Having the steady state probabilities $\{\bar{\pi}_q\}$ in Proposition 1 and the set of transitions $\mathcal{L}$ in Table I, we are now ready to derive the MGF of AoI in the following theorem.

Theorem 1. *The MGF of AoI of source 1 for the LCFS-WP queueing discipline is given by*

$$\overset{\text{WP}}{M}_1(\bar{s}) = \frac{\rho_1(1+\rho-\bar{s})\sum_{q\in\mathrm{r}_1/\{1\}}\bar{\pi}_q + \bar{v}_{10}^s\rho_1(1-\bar{s})}{(1-\bar{s})\Big[(1-\bar{s})(\rho-\bar{s}) - \rho_{-1}\Big]}, \tag{13}$$

where $\bar{s} = \frac{s}{\mu}$ and $\bar{v}_{10}^s$ is given by

$$\bar{v}_{10}^s = \frac{\rho_1}{\rho_{-1}}\sum_{j=0}^{B-1}\frac{\bar{\pi}_{2j+2}}{\prod_{h=0}^{j}c_{2h}^s}\left(\frac{\mu\rho_{-1}}{1-\bar{s}}\right)^j, \tag{14}$$

where the set $\{c_0^s, c_2^s, \cdots, c_{2B}^s\}$ is defined as

$$c_{2h}^s = \begin{cases} \lambda - s, & h = B, \\ \eta + \lambda - s - \dfrac{\mu\eta\lambda_{-1}}{c_{2h+2}^s(\mu - s)}, & 1 \leq h \leq B-1, \\ \dfrac{(\mu-s)(\eta-s)}{\mu\lambda_{-1}} - \dfrac{\eta}{c_2^s}, & h = 0. \end{cases} \tag{15}$$

Proof: See Appendix A. ∎

Note that the MGF of AoI for source $i \in \{2, 3, \cdots, N\}$ can be obtained directly using (13) by replacing λ_1 with λ_i (which results in replacing $\{\lambda_{-1}, \rho_1, \rho_{-1}\}$ with $\{\lambda_{-i}, \rho_i, \rho_{-i}\}$ as well). This argument applies to all the following results.

Corollary 1. *When $\rho_{-1} = 0$ (i.e., $\rho_1 = \rho$), $\overset{\text{WP}}{M}_1(\bar{s})$ in (13) reduces to the following MGF of AoI derived in [20, Theorem 1] for the case where an EH-powered transmitter with a single source employs the LCFS-WP queueing discipline*

$$\overset{\text{WP}}{M}_1(\bar{s}) = \frac{\rho\bar{\pi}_1\Big[\bar{s}^2\theta - \bar{s}\theta(1+\rho+\beta) + \beta(1+\theta+\theta\rho)\Big]}{(1-\bar{s})^2(\rho-\bar{s})(\beta-\bar{s})}, \tag{16}$$

where θ can be expressed as

$$\theta = \begin{cases} B, & \text{if } \rho = \beta, \\ \dfrac{\beta\left(\beta^B - \rho^B\right)}{\rho^B\left(\beta - \rho\right)}, & \text{otherwise.} \end{cases} \tag{17}$$

Proof: When $\rho_{-1} = 0$, we first note from (15) that we have: $c_{2h}^s = \eta + \lambda - s, 1 \leq h \leq B-1$, and $c_0^s = \infty$. As a result, $\bar{v}_{10}^s$ reduces to $\dfrac{\rho_1 \bar{\pi}_2}{(1-\bar{s})(\beta - \bar{s})}$. The final expression in (16) can be obtained by defining $\sum_{q \in \mathrm{r}_1/\{1\}} \bar{\pi}_q = \theta \bar{\pi}_1$ and substituting $\bar{\pi}_2$ from Proposition 1 as $\frac{\beta}{\rho}\bar{\pi}_1$. ■

Corollary 2. *The average AoI of source 1 under the LCFS-WP queueing discipline is given by:*

$$\overset{\mathrm{WP}}{\Delta}_{1,1} = \frac{1+\rho}{\mu\rho_1} + \frac{\sum_{q\in \mathrm{r}_2}\bar{\pi}_q}{\mu} + \frac{\bar{\pi}_1}{c_0\mu\rho_{-1}} + \sum_{j=1}^{B} \frac{\bar{\pi}_{2j}\left(\mu\rho_{-1}\right)^{j-1}}{\prod_{h=0}^{j} c_{2h}} + \sum_{j=0}^{B-1} \frac{\bar{\pi}_{2j+3}\left(\mu\rho_{-1}\right)^{j-1}}{\prod_{h=0}^{j} c_{2h}}, \tag{18}$$

where the set $\{c_0, c_2, \cdots, c_{2B}\}$ is defined as

$$c_{2h} = \begin{cases} \lambda, & h = B, \\ \eta\left(1 - \dfrac{\lambda_{-1}}{c_{2h+2}}\right) + \lambda, & 1 \leq h \leq B-1, \\ \eta\left(\dfrac{1}{\lambda_{-1}} - \dfrac{1}{c_2}\right), & h = 0. \end{cases} \tag{19}$$

Proof: The result can be obtained from either the first derivative of the MGF of AoI in Theorem 1 or the solution of the set equations in (3) as in (8). ■

Corollary 3. *For the single source case where $\rho_{-1} = 0$ and $\rho = \rho_1$, $\overset{\mathrm{WP}}{\Delta}_{1,1}$ in (18) reduces to*

$$\overset{\mathrm{WP}}{\Delta}_{1,1} = \begin{cases} \dfrac{2B\rho^2 + 2(1+B)\rho + B + 2}{\mu\left[B\rho^2 + (1+B)\rho\right]}, & \text{if } \rho = \beta, \\ \dfrac{\beta^{B+2}\left(2\rho^2+2\rho+1\right) - \rho^{B+2}\left(2\beta^2+2\beta+1\right)}{\mu\left[\beta^{B+2}\left(\rho^2+\rho\right) - \rho^{B+2}\left(\beta^2+\beta\right)\right]}, \end{cases} \tag{20}$$

where the second case in (20) holds when $\rho \neq \beta$. Note that the expression of $\overset{\mathrm{WP}}{\Delta}_{1,1}$ in (20) is identical to the average AoI expression derived in [17, Theorem 3] under the LCFS-WP queueing discipline (for the case of having an EH-powered transmitter with a single source).

Proof: We note from (19) that when $\rho_{-1} = 0$, we have $c_{2h} = \eta + \lambda, 1 \leq h \leq B-1$, and $c_0 = \infty$. Thus, $\overset{\mathrm{WP}}{\Delta}_{1,1}$ in (18) reduces to: $\overset{\mathrm{WP}}{\Delta}_{1,1} = \dfrac{1+\rho}{\mu\rho_1} + \dfrac{\sum_{q\in\mathrm{r}_2}\bar{\pi}_q}{\mu} + \dfrac{\bar{\pi}_1 + \bar{\pi}_3}{\eta}$. The final expression in (20) can be obtained by substituting $\{\bar{\pi}_q\}$ from Proposition 1, followed by some algebraic simplifications. ■

Corollary 4. *When $\beta \to \infty$, $\overset{\mathrm{WP}}{\Delta}_{1,1}$ in (18) reduces to*

$$\lim_{\beta\to\infty} \overset{\mathrm{WP}}{\Delta}_{1,1} = \frac{1+\rho}{\mu\rho_1} + \frac{\rho}{\mu(1+\rho)}. \tag{21}$$

Note that the expression in (21) is identical to the average AoI expression in the case where a non-EH transmitter with multiple sources employs the LCFS-WP queueing discipline. Further, by setting ρ_1 in (21) to ρ, we obtain $\lim_{\beta\to\infty} \overset{\mathrm{WP}}{\Delta}_{1,1} = \dfrac{2\rho^2+2\rho+1}{\mu\left(\rho^2+\rho\right)}$, which is the average AoI expression derived in [27] for the M/M/1/1 case (where a non-EH transmitter with single source employing the LCFS-WP queueing discipline was considered).

Proof: The result follows from noting that: $\lim_{\beta\to\infty} \dfrac{\bar{\pi}_1}{c_0\mu\rho_{-1}} = \lim_{\beta\to\infty} \sum_{j=1}^{B} \dfrac{\bar{\pi}_{2j}\left(\mu\rho_{-1}\right)^{j-1}}{\prod_{h=0}^{j} c_{2h}} = \lim_{\beta\to\infty} \sum_{j=0}^{B-1} \dfrac{\bar{\pi}_{2j+3}\left(\mu\rho_{-1}\right)^{j-1}}{\prod_{h=0}^{j} c_{2h}} = 0$ and $\lim_{\beta\to\infty} \dfrac{\sum_{q\in\mathrm{r}_2}\bar{\pi}_q}{\mu} = \dfrac{\rho}{\mu(1+\rho)}$. ■

B. LCFS-PS Queueing Discipline

Fig. 2b depicts the Markov chain representing the discrete state of the system under the LCFS-PS queueing discipline, where the structure of $\mathcal{Q}$ is similar to the one associated with the LCFS-WP queueing discipline. Further, the set of transitions in the LCFS-PS queueing discipline can be constructed using Tables I and II. The subset of transitions in Table II refers to the event of having a new arriving update packet at the transmitter node while its server is serving another update packet. According to the mechanism of the LCFS-PS queueing discipline, the status update that is currently being served will be discarded, and the new arrival will enter service upon its arrival. From (4), we note that the self-transitions do not impact the values of the steady state probabilities $\{\bar{\pi}_q\}$, and hence $\{\bar{\pi}_q\}$ in this case can be obtained using Proposition 1. That said, the MGF of $\Delta_1(t)$ is provided in the next theorem.

Theorem 2. *The MGF of AoI of source 1 for the LCFS-PS queueing discipline is given by*

$$\overset{\mathrm{PS}}{M}_1(\bar{s}) = \frac{\rho_1\left(1 - \bar{\pi}_1 + \bar{v}_{10}^s\right)}{(1-\bar{s})(\rho - \bar{s}) - \rho_{-1}}, \tag{22}$$

where $\bar{v}_{10}^s$ is given by

$$\bar{v}_{10}^s = \frac{\mu\rho_1}{1+\rho-\bar{s}} \sum_{j=0}^{B-1} \frac{\bar{\pi}_{2j+2} + \bar{\pi}_{2j+3}}{\prod_{h=0}^{j} c_{2h}^s} \left(\frac{\mu\rho_{-1}}{1-\bar{s}}\right)^{j-1}, \tag{23}$$

where the set $\{c_0^s, c_2^s, \cdots, c_{2B}^s\}$ is defined as in (15).

Proof: See Appendix B. ■

Corollary 5. *When $\rho_{-1} = 0$ (i.e., $\rho_1 = \rho$), $\overset{\mathrm{PS}}{M}_1(\bar{s})$ in (22) reduces to the following MGF of AoI derived in [20, Theorem 3] for the case where an EH-powered transmitter with a single source employs the LCFS-PS queueing discipline*

$$\overset{\mathrm{PS}}{M}_1(\bar{s}) = \frac{\bar{\pi}_1\left[\bar{s}^2\theta - \bar{s}\theta(1+\rho+\beta) + \beta(1+\theta+\theta\rho)\right]}{\rho^{-1}(1+\rho)^{-1}(1-\bar{s})(\rho-\bar{s})(1+\rho-\bar{s})(\beta-\bar{s})}, \tag{24}$$

where θ is given by (17).

Corollary 6. *The average AoI of source 1 under the LCFS-PS queueing discipline is given by*

$$\overset{\mathrm{PS}}{\Delta}_{1,1} = \frac{1+\rho}{\mu\rho_1} + \frac{\bar{\pi}_1}{c_0\mu\rho_{-1}} + \sum_{j=1}^{B} \frac{\bar{\pi}_{2j}\left(\mu\rho_{-1}\right)^{j-1}}{\prod_{h=0}^{j} c_{2h}} + \frac{1+\rho_{-1}}{1+\rho} \sum_{j=0}^{B-1} \frac{\bar{\pi}_{2j+3}\left(\mu\rho_{-1}\right)^{j-1}}{\prod_{h=0}^{j} c_{2h}}, \tag{25}$$

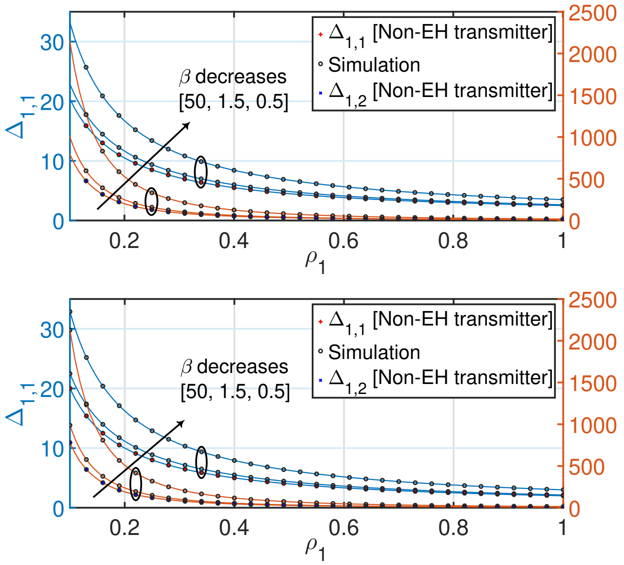

Fig. 3. Impact of β on the achievable AoI performance: (*first*) LCFS-WP queueing discipline, and (*second*) LCFS-PS queueing discipline. N can be arbitrary chosen, and We use $\rho = 1$ and $B = 2$.

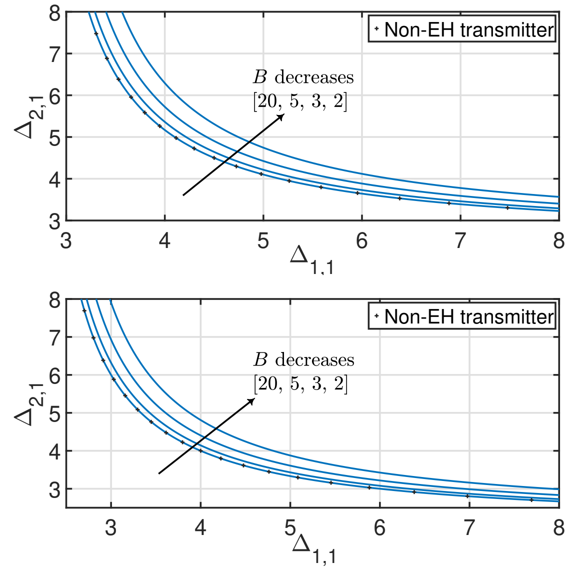

Fig. 4. Impact of B on the achievable pairs of average AoI when $N = 2$: (*first*) LCFS-WP queueing discipline, and (*second*) LCFS-PS queueing discipline. We use $\rho = 1$ and $\beta = 1.5$.

where the set $\{c_0, c_2, \cdots, c_{2B}\}$ is defined as in (19).

Corollary 7. *For the single source case where $\rho_{-1} = 0$ and $\rho = \rho_1$, $\overset{\text{PS}}{\Delta}_{1,1}$ in (25) reduces to:* $\overset{\text{PS}}{\Delta}_{1,1} =$

$$\begin{cases} \dfrac{B\rho^3 + (3B+1)\,\rho^2 + (3B+4)\,\rho + B + 2}{\mu\rho\,(1+\rho)\,(\rho B + B + 1)}, & \text{if } \rho = \beta, \\ \dfrac{\beta^{B+2}\,(1+\rho)^3 - \rho^{B+2}\big[\,(\beta^2+\beta)\,(\rho+2) + 1 + \rho\big]}{\mu\,(1+\rho)\,\big[\beta^{B+2}\,(\rho^2+\rho) - \rho^{B+2}\,(\beta^2+\beta)\,\big]}, \end{cases} \tag{26}$$

where the second case in (26) holds when $\rho \neq \beta$. Note that the expression of $\overset{\text{PS}}{\Delta}_{1,1}$ in (26) is identical to the average AoI expression derived in [20, Corollary 3] under the LCFS-PS queueing discipline (for the case of having an EH-powered transmitter with a single source).

Corollary 8. *When $\beta \to \infty$, $\overset{\text{PS}}{\Delta}_{1,1}$ in (25) reduces to*

$$\lim_{\beta\to\infty} \overset{\text{PS}}{\Delta}_{1,1} = \frac{1+\rho}{\mu\rho_1}. \tag{27}$$

Note that the expression in (27) is identical to the average AoI expression derived in [8, Theorem 2(a)] for the case where a non-EH transmitter with multiple sources employs the LCFS-PS queueing discipline.

Remark 1. *Note that from Corollaries 2 and 6, we have*

$$\overset{\text{WP}}{\Delta}_{1,1} - \overset{\text{PS}}{\Delta}_{1,1} = \frac{\sum_{q\in\mathbb{r}_2} \bar{\pi}_q}{\mu} + \frac{\rho_1}{1+\rho} \sum_{j=0}^{B-1} \frac{\bar{\pi}_{2j+3}\,(\mu\rho_{-1})^{j-1}}{\prod_{h=0}^{j} c_{2h}}. \tag{28}$$

Since the set $\{c_0, c_2, \cdots, c_{2B}\}$ contains positive real numbers, we observe from (28) that $\overset{\text{WP}}{\Delta}_{1,1} - \overset{\text{PS}}{\Delta}_{1,1} \geq 0$ for any choice of values of the system parameters. This, in turn, indicates the superiority of the LCFS-PS queueing discipline over LCFS-WP in terms of the achievable average AoI at the destination node.

Remark 2. *Let $\overset{\text{D}}{\Delta}_{i,j}$ denote the j-th moment of source i's AoI under queueing discipline* D. *Then, one can deduce from Theorems 1 and 2 that $\overset{\text{PS}}{\Delta}_{1,2} \leq \overset{\text{WP}}{\Delta}_{1,2}$ for any choice of system parameter values.*

V. Numerical Results

In this section, we study the impact of the system design parameters on the achievable AoI performance under each of the two queueing disciplines considered in this paper. We use $\mu = 1$ throughout this section. In Fig 3, we first verify the accuracy of the analytical expressions of the first and second moments of AoI for each queueing discipline (obtained using the MGFs derived in Theorems 1 and 2) by comparing them to their simulated counterparts (obtained numerically using [9, Theorem 1]). We then study the impact of battery capacity (B) on the achievable pairs of average AoI in Fig. 4 when $N = 2$ and ρ is fixed. From Figs. 3 and 4, we observe that increasing B or β improves the AoI performance of each queueing discipline until it converges to its counterpart with a non-EH transmitter (as stated in Corollaries 4 and 8). In particular, the likelihood that the battery queue is empty upon the arrival of a new status update at the transmitter decreases with the increment of B or β. As a result, the likelihood of delivering new arriving updates to the destination increases with B or β, which leads to the improvement in the AoI performance.

In Figs. 5 and 6, we compare the two queueing disciplines studied in this paper in terms of: i) the average sum-AoI $\Delta_{1,1} + \Delta_{2,1}$, and ii) the Jain's fairness index, which is defined as $\text{JFI} = \dfrac{\left(\sum_{i=1}^{N} \Delta_{i,1}\right)^2}{N\sum_{i=1}^{N} \Delta_{i,1}^2}$ [28]. Note that the JFI $\in \left[N^{-1}, 1\right]$ is a measure of the fairness between the achievable average AoI values by different sources such that JFI $= 1$ when the average AoI values of different sources are equal (the best scenario with respect to fairness). First, we observe from Fig. 5 the superiority of the LCFS-PS queueing discipline over

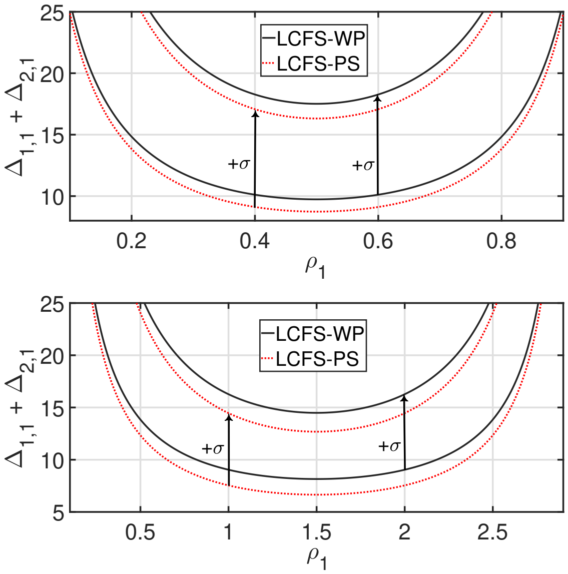

Fig. 5. Comparison between the LCFS-WP and LCFS-PS queueing disciplines in terms of the achievable average sum-AoI for $\rho = 1$ (*first*) and 3 (*second*). We use $N = 2$, $B = 2$ and $\beta = 1.5$.

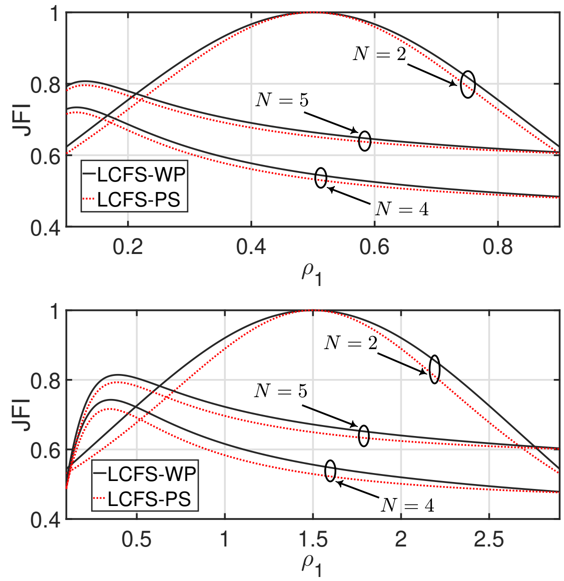

Fig. 6. Comparison between the LCFS-WP and LCFS-PS queueing disciplines in terms of the Jain's fairness index for $\rho = 1$ (*first*) and 3 (*second*). We use $B = 2$ and $\beta = 1.5$. For $N \in \{4, 5\}$, we set $\rho_2 = 0.1(\rho - \rho_1)$ and $\rho_i = \frac{0.9}{N-2}(\rho - \rho_1)$, $3 \le i \le N$.

the LCFS-WP one in terms of the achievable average sum-AoI (which supports our arguments in Remark 1). However as evident from Fig. 6, such a superiority of the LCFS-PS queueing discipline comes at the expense of having unfair achievable average AoI values among different sources. Second, as was the case in [20] for single-source systems with an EH-powered transmitter node, we observe from Fig. 5 that the standard deviation of AoI σ associated with each queueing discipline in multi-source systems is relatively large with respect to the average value. This highlights the unreliability of implementing multi-source status update systems based on just the average AoI, and the importance of incorporating the higher moments of AoI in the design/optimization of such systems. This insight also demonstrates the significance of the analytical distributional properties of AoI derived in this paper.

VI. Conclusion

This paper analytically characterized the distributional properties of AoI in multi-source updating systems powered by EH, where an EH-powered transmitter sends status updates about several observed physical processes to a destination. In particular, we used the SHS framework to derive the MGF/average of AoI in closed-form under both non-preemptive (LCFS-WP) and preemptive in service (LCFS-PS) queueing disciplines. Our analytical results allowed us to obtain several useful insights regarding the achievable AoI performance under the considered queueing disciplines. For instance, the gap between the achievable average AoI performances by the considered two queueing disciplines was characterized in closed-form as a function of the system parameters. Several key system design insights were also drawn from our numerical results. For instance, our results revealed that the superiority of the LCFS-PS queueing discipline over the LCFS-WP one in terms of the achievable average sum-AoI comes at the expense of having unfair average AoI values of different sources. They also revealed that it is necessary to incorporate the higher moments of AoI in the implementation/optimization of multi-source real-time status updates systems rather than just relying on its average value.

Appendix

A. Proof of Theorem 1

Using Table I, the set of equations in (6) can be expressed as

$$q_1: \quad (\eta - s)\,[\bar{v}^s_{10}, \bar{v}^s_{11}] = \mu[\bar{v}^s_{31}, \bar{\pi}_3], \tag{29}$$

$$q_2: \quad (\eta + \lambda - s)\,[\bar{v}^s_{20}, \bar{v}^s_{21}] = \mu[\bar{v}^s_{51}, \bar{\pi}_5] + \eta[\bar{v}^s_{10}, \bar{\pi}_1], \tag{30}$$

$$q_{2k}, 2 \le k \le B-1: \quad (\eta + \lambda - s)\,[\bar{v}^s_{2k,0}, \bar{v}^s_{2k,1}] = \mu[\bar{v}^s_{2k+3,1}, \bar{\pi}_{2k+3}] + \eta[\bar{v}^s_{2k-2,0}, \bar{\pi}_{2k-2}], \tag{31}$$

$$q_{2B}: \quad (\lambda - s)\,[\bar{v}^s_{2B,0}, \bar{v}^s_{2B,1}] = \eta[\bar{v}^s_{2B-2,0}, \bar{\pi}_{2B-2}], \tag{32}$$

$$q_{2k+1}, 1 \le k \le B: \quad (\mu - s)\,[\bar{v}^s_{2k+1,0}, \bar{v}^s_{2k+1,1}] = \lambda_1[\bar{v}^s_{2k,0}, \bar{\pi}_{2k}] + \lambda_2[\bar{v}^s_{2k,0}, \bar{v}^s_{2k,0}]. \tag{33}$$

Summing the set of equations in (29)-(32) gives

$$(\lambda - s) \sum_{q \in \mathrm{r}_1} \bar{v}^s_{q0} = \mu \sum_{q \in \mathrm{r}_2} \bar{v}^s_{q1} + \lambda \bar{v}^s_{10}. \tag{34}$$

Further, by summing the set of equations in (33), we get

$$(\mu - s) \sum_{q \in \mathrm{r}_2} \bar{v}^s_{q0} = \lambda \sum_{q \in \mathrm{r}_1} \bar{v}^s_{q0} - \lambda \bar{v}^s_{10}. \tag{35}$$

$$(\mu - s) \sum_{q \in \mathrm{r}_2} \bar{v}^s_{q1} = \lambda_1 \sum_{q \in \mathrm{r}_1/\{1\}} \bar{\pi}_q + \lambda_2 \sum_{q \in \mathrm{r}_1/\{1\}} \bar{v}^s_{q0}. \tag{36}$$

From (9), the MGF of AoI of source 1 at the destination can be evaluated as

$$\overset{\mathrm{WP}}{M}_1(\bar{s}) = \sum_{q \in \mathrm{r}_1 \cup \mathrm{r}_2} \bar{v}^s_{q0} \overset{(\mathrm{a})}{=} \frac{(\lambda + \mu - s) \sum_{q \in \mathrm{r}_1} \bar{v}^s_{q0} - \lambda \bar{v}^s_{10}}{\mu - s},$$
$$\overset{(\mathrm{b})}{=} \frac{\rho_1 (1 + \rho - \bar{s}) \sum_{q \in \mathrm{r}_1/\{1\}} \bar{\pi}_q + \bar{v}^s_{10} \rho_1 (1 - \bar{s})}{(1 - \bar{s}) \Big[(1 - \bar{s})(\rho - \bar{s}) - \rho_{-1} \Big]}, \tag{37}$$

where step (a) follows from substituting (35) into (37), and step (b) follows from obtaining $\sum_{q\in \mathrm{r}_1} \bar{v}^s_{q0}$ from (34)-(36) as $\frac{\rho_1 \sum_{q\in \mathrm{r}_1/\{1\}} \bar{\pi}_q + \bar{v}^s_{10}(\rho_1-\rho\bar{s})}{(1-\bar{s})(\rho-\bar{s})-\rho_{-1}}$ and substituting it into (37). Now, what only remains is to show how $\bar{v}^s_{10}$ can be expressed as in (14). From (32), $\bar{v}^s_{2B,0}$ can be expressed as

$$\bar{v}^s_{2B,0} = \frac{\eta\bar{v}^s_{2B-2,0}}{c^s_{2B}} \tag{38}$$

where $c^s_{2B} = \lambda - s$. Substituting $k = B-1$ in (31), $\bar{v}^s_{2B-2,0}$ can be expressed as

$$\bar{v}^s_{2B-2,0} = \frac{\eta\bar{v}^s_{2B-4,0}}{c^s_{2B-2}} + \frac{\mu\lambda_1\bar{\pi}_{2B}}{c^s_{2B-2}(\mu-s)}, \tag{39}$$

where $\bar{v}^s_{2B+1,1}$ and $\bar{v}^s_{2B,0}$ were respectively substituted from (33) and (38), and $c^s_{2B-2} = \eta+\lambda-s-\dfrac{\mu\eta\lambda_2}{c^s_{2B}(\mu-s)}$. Repeated application of (31) gives

$$\bar{v}^s_{2k,0} = \frac{\eta\bar{v}^s_{2k-2}}{c^s_{2k}} + \frac{\rho_1}{\rho_{-1}}\sum_{j=1}^{B-k}\frac{\bar{\pi}_{2(k+j)}}{\prod_{h=1}^{j} c^s_{2(k+h-1)}}\left(\frac{\mu\rho_{-1}}{1-\bar{s}}\right)^j, \tag{40}$$

$$\bar{v}^s_{20} = \frac{\eta\bar{v}^s_{10}}{c^s_2} + \frac{\rho_1}{\rho_{-1}}\sum_{j=1}^{B-1}\frac{\bar{\pi}_{2(j+1)}}{\prod_{h=1}^{j} c^s_{2h}}\left(\frac{\mu\rho_{-1}}{1-\bar{s}}\right)^j, \tag{41}$$

where $2 \le k \le B$ and $\{\bar{c}^s_{2h}\}$ is defined in (15). Finally, $\bar{v}^s_{10}$ in (14) can be obtained by solving (29) and (41) while substituting $\bar{v}^s_{31}$ from (33). ■

B. *Proof of Theorem 2*

We first note that the set of equations in (6) corresponding to the states in r_1 are given by (29)-(32), and hence $\sum_{q\in \mathrm{r}_1} \bar{v}^s_{q0}$ can be expressed as in (34). Regarding the states in r_2, we have

$$\begin{aligned}&q_{2k+1}, 1 \le k \le B: \quad (\mu-s)\,\bar{v}^s_{2k+1,0} = \lambda\bar{v}^s_{2k,0},\\ &(\lambda+\mu-s)\,\bar{v}^s_{2k+1,1} = \lambda_2(\bar{v}^s_{2k,0} + \bar{v}^s_{2k+1,0}) + \lambda_1(\bar{\pi}_{2k} + \bar{\pi}_{2k+1}).\end{aligned} \tag{42}$$

We observe from (42) that $\sum_{q\in \mathrm{r}_2} \bar{v}^s_{q0}$ is given by (35) and $\sum_{q\in \mathrm{r}_2} \bar{v}^s_{q1}$ can be expressed as

$$(\lambda+\mu-s)\sum_{q\in \mathrm{r}_2}\bar{v}^s_{q1} = \lambda_2\sum_{q\in \mathcal{Q}/\{1\}}\bar{v}^s_{q0} + \lambda_1(1-\bar{\pi}_1). \tag{43}$$

Hence, the MGF of AoI of source 1 at the destination can be evaluated as

$$\begin{aligned}\overset{\mathrm{PS}}{M}_1(\bar{s}) = \sum_{q\in \mathrm{r}_1\cup \mathrm{r}_2}\bar{v}^s_{q0} &\overset{(a)}{=} \frac{(\lambda+\mu-s)\sum_{q\in \mathrm{r}_1}\bar{v}^s_{q0} - \lambda\bar{v}^s_{10}}{\mu-s},\\ &\overset{(b)}{=} \frac{\rho_1(1-\bar{\pi}_1+\bar{v}^s_{10})}{(1-\bar{s})(\rho-\bar{s})-\rho_{-1}},\end{aligned} \tag{44}$$

where step (a) follows from substituting (35) into (44), and step (b) follows from obtaining $\sum_{q\in \mathrm{r}_1} \bar{v}^s_{q0}$ from (34), (35) and (43) as $\frac{\rho_1(1-\bar{\pi}_1)(1-\bar{s})+\bar{v}^s_{10}(\rho_1-\rho\bar{s})(1+\rho-\bar{s})}{(1+\rho-\bar{s})[(1-\bar{s})(\rho-\bar{s})-\rho_{-1}]}$ and substituting it into (44). Finally, $\bar{v}^s_{10}$ in (23) can be obtained by following similar steps as in (38)-(41). ■

References

[1] M. A. Abd-Elmagid, N. Pappas, and H. S. Dhillon, "On the role of age of information in the Internet of things," *IEEE Commun. Magazine*, vol. 57, no. 12, pp. 72–77, Dec. 2019.

[2] S. Kaul, R. Yates, and M. Gruteser, "Real-time status: How often should one update?" in *Proc., IEEE INFOCOM*, 2012.

[3] R. D. Yates and S. Kaul, "Real-time status updating: Multiple sources," in *Proc., IEEE Intl. Symposium on Information Theory*, 2012.

[4] M. Moltafet, M. Leinonen, and M. Codreanu, "On the age of information in multi-source queueing models," *IEEE Trans. on Commun.*, vol. 68, no. 8, pp. 5003–5017, Aug. 2020.

[5] N. Pappas, J. Gunnarsson, L. Kratz, M. Kountouris, and V. Angelakis, "Age of information of multiple sources with queue management," in *Proc., IEEE Intl. Conf. on Commun. (ICC)*, 2015.

[6] A. Kosta, N. Pappas, A. Ephremides, and V. Angelakis, "Age of information performance of multiaccess strategies with packet management," *Journal of Commun. and Networks*, vol. 21, no. 3, pp. 244–255, 2019.

[7] N. Akar and O. Dogan, "Discrete-time queueing model of age of information with multiple information sources," *IEEE Internet of Things Journal*, vol. 8, no. 19, pp. 14 531–14 542, Oct. 2021.

[8] R. D. Yates and S. K. Kaul, "The age of information: Real-time status updating by multiple sources," *IEEE Trans. on Info. Theory*, vol. 65, no. 3, pp. 1807–1827, Mar. 2019.

[9] R. D. Yates, "The age of information in networks: Moments, distributions, and sampling," *IEEE Trans. on Info. Theory*, vol. 66, no. 9, pp. 5712–5728, Sept. 2020.

[10] J. P. Hespanha, "Modelling and analysis of stochastic hybrid systems," *IEE Proceedings-Control Theory and Applications*, vol. 153, no. 5, pp. 520–535, Sept. 2006.

[11] A. Maatouk, M. Assaad, and A. Ephremides, "On the age of information in a csma environment," *IEEE/ACM Trans. on Networking*, vol. 28, no. 2, pp. 818–831, Apr. 2020.

[12] M. Moltafet, M. Leinonen, and M. Codreanu, "Average AoI in multi-source systems with source-aware packet management," *IEEE Trans. on Commun.*, vol. 69, no. 2, pp. 1121–1133, Feb. 2021.

[13] A. Javani, M. Zorgui, and Z. Wang, "Age of information for multiple-source multiple-server networks," 2021, available online: arxiv.org/abs/2106.07247.

[14] M. Moltafet, M. Leinonen, and M. Codreanu, "Moment generating function of the AoI in a two-source system with packet management," *IEEE Wireless Commun. Letters*, vol. 10, no. 4, pp. 882–886, Apr. 2021.

[15] R. D. Yates, "Lazy is timely: Status updates by an energy harvesting source," in *Proc., IEEE Intl. Symposium on Information Theory*, 2015.

[16] X. Zheng, S. Zhou, Z. Jiang, and Z. Niu, "Closed-form analysis of non-linear age of information in status updates with an energy harvesting transmitter," *IEEE Trans. on Wireless Commun.*, vol. 18, no. 8, pp. 4129–4142, Aug. 2019.

[17] S. Farazi, A. G. Klein, and D. R. Brown, "Average age of information for status update systems with an energy harvesting server," in *Proc., IEEE INFOCOM Workshops*, 2018.

[18] S. Farazi, A. G. Klein, and D. R. Brown, "Age of information in energy harvesting status update systems: When to preempt in service?" in *Proc., IEEE Intl. Symposium on Information Theory*, 2018.

[19] J. Doncel, "Age of information of a server with energy requirements," *PeerJ Computer Science*, vol. 7, p. e354, Mar. 2021.

[20] M. A. Abd-Elmagid and H. S. Dhillon, "Closed-form characterization of the MGF of AoI in energy harvesting status update systems," *IEEE Trans. on Info. Theory*, to appear.

[21] B. T. Bacinoglu, E. T. Ceran, and E. Uysal-Biyikoglu, "Age of information under energy replenishment constraints," in *Proc., Information Theory and its Applications (ITA)*, 2015.

[22] X. Wu, J. Yang, and J. Wu, "Optimal status update for age of information minimization with an energy harvesting source," *IEEE Trans. on Green Commun. and Networking*, vol. 2, no. 1, pp. 193–204, Mar. 2018.

[23] A. Arafa, J. Yang, S. Ulukus, and H. V. Poor, "Age-minimal transmission for energy harvesting sensors with finite batteries: Online policies," *IEEE Trans. on Info. Theory*, vol. 66, no. 1, pp. 534–556, Jan. 2020.

[24] M. A. Abd-Elmagid, H. S. Dhillon, and N. Pappas, "A reinforcement learning framework for optimizing age of information in RF-powered communication systems," *IEEE Trans. on Commun.*, vol. 68, no. 8, pp. 4747 – 4760, Aug. 2020.

[25] M. A. Abd-Elmagid, H. S. Dhillon, and N. Pappas, "AoI-optimal joint sampling and updating for wireless powered communication systems," *IEEE Trans. on Veh. Technology*, vol. 69, no. 11, pp. 14 110–14 115, Nov. 2020.

[26] M. A. Abd-Elmagid and H. S. Dhillon, "Age of information in multi-source updating systems powered by energy harvesting," under revision at *IEEE Journal on Selected Areas in Info. Theory.*

[27] M. Costa, M. Codreanu, and A. Ephremides, "On the age of information in status update systems with packet management," *IEEE Trans. on Info. Theory*, vol. 62, no. 4, pp. 1897–1910, Apr. 2016.

[28] R. Jain, D.-M. Chiu, and W. Hawe, "A quantitative measure of fairness and discrimination for resource allocation in shared computer systems," *DEC Research Repor, Technical Report TR-301*, Sept. 1984.